Siting and Sizing Resilience Hubs for Grid and Community Resilience During Heat Waves

Alex Farley, Hollis Belnap, Masood Parvania
Department of Electrical and Computer Engineering, The University of Utah, Salt Lake City, UT 84112 USA
E-mails: {alex.farley, hollis.belnap, masood.parvania}@utah.edu

Abstract

The increased intensity and frequency of heat waves are impacting communities and power grid operations worldwide. Resilience hubs can provide communities with several essential services and resources, including community-oriented resilience to heat waves. This paper presents a framework for siting resilience hubs to reduce community vulnerability to heat waves based on air conditioning systems, socioeconomic status, and urban heating effects. Additionally, this paper utilizes a mixed-integer linear programming model to design a resilience hub's energy system to ensure it can meet the service demands of its surrounding community, considering different outage scenarios during a heat wave. An economic analysis discusses the cost-effectiveness of different resilience hub designs. A case study reports the optimal sites and designs of resilience hubs in the metro area of Salt Lake City, Utah, to reduce community vulnerability to heat waves.

1. Introduction

1.1. Background and Literature Review

Climate change has increased the intensity and frequency of heat waves across the globe. In the U.S., heat wave season is now 49 days longer than it was in the 1960s, with a statistically significant increase in the frequency of heat wave events [1]. In 2023 and 2024, many areas have recorded their highest temperatures ever. These extreme temperatures present a public health risk. High indoor temperatures have been shown to affect respiratory health, diabetes management, and dementia symptoms [2]. Over 2,300 people died in the U.S. due to heat-related illnesses in 2023, the highest number recorded in 45 years [3].

Heat waves also pose an especially difficult challenge for power system operations. Generally, peak annual electricity demand corresponds to the year's hottest days. Extreme temperatures also strain power grid equipment and cause transmission lines to reach operating limits, constraining power flow and further reducing capacity and flexibility. In extreme cases, grid operators have to administer rolling outages to maintain power balance. This can be especially dangerous because air conditioning systems, the public's primary response to heat waves, are inoperable without power.

The inequitable impacts of heat waves across communities are becoming increasingly apparent. Older homes, typically owned by lower-income individuals, are disproportionately less weatherized, making them more susceptible to high indoor temperatures during heat waves. Similarly, low-income individuals are more likely to make efforts to limit energy consumption as they spend a larger percentage of their income on energy costs, resulting in higher indoor temperatures and a higher risk of heat-related illness [4]. The effects of heat waves are also exacerbated intra-city, where local infrastructure can intensify heat waves through the urban heating effect. In [5], it was found that low-income neighborhoods experience elevated heat exposure compared to more wealthy neighborhoods in 72% of surveyed American cities.

A handful of works evaluate the nexus of heat waves, power system operation, and community impacts. For instance, a methodology to assess the risks of power outages on a nodal basis in the power distribution system during heat waves is presented in [6]. This methodology is further developed in [7], integrating overheating risk into distribution system planning models. In [8], it was found air conditioning failure can quickly lead to dangerously high indoor temperatures. The spatiotemporal distribution of power outages in counties in the U.S. was analyzed against social vulnerability metrics, finding a statistically significant correlation between disadvantaged communities and more long-duration power outages in [9]. A methodology to quantify multi-dimensional community vulnerability to power outages under a single metric using principal component analysis and the L2 norm was presented in [10]. The potential for energy storage systems to enhance energy access under varying ownership structures during different outage conditions using resource adequacy analysis was studied in [11].

Studies have shown the power system's critical

URI: https://hdl.handle.net/10125/109198
978-0-9981331-8-8
(CC BY-NC-ND 4.0)

role in exacerbating or mitigating the effects of heat waves. In practice, cities across the U.S. have "cooling zone" programs, where they actively open public buildings with HVAC systems to the public to find reprieve and safe indoor temperatures. Nonetheless, no work has analyzed how a resilience hub, a community-oriented facility with a resilient energy system for providing services during normal operations and extreme weather events, can be designed to enhance community resilience to heat waves.

1.2. Contributions and Paper Structure

This paper presents a framework to site and design resilience hubs to mitigate the inequitable effects of heat waves and improve overall community resilience, as summarized in Fig. 1. First, the vulnerability of a given community, considering their home air conditioning capabilities, socioeconomic status, and local urban heating effect, is quantified. Next, an optimization model is used to site resilience hubs within a discrete set of public locations to mitigate community vulnerability to heat waves. With this, hub thermal simulations provide the air conditioning system requirements needed to maintain a safe indoor temperature during a heat wave. A second optimization model then determines the minimum necessary solar PV capacity, energy storage capacity, and initial state of charge to serve the resilience hub's electricity demand during various outage scenarios. An economic assessment is also included for the design of the hub's energy system. This paper provides a novel approach developed to assist a variety of local governments, urban planners, and organizations in developing strategies to mitigate the inequitable impacts of heat waves on communities by retrofitting existing public infrastructure.

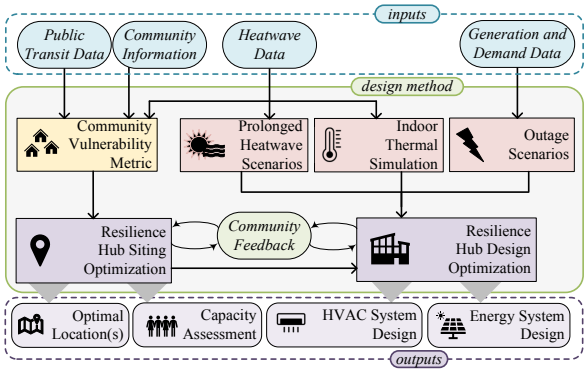

Figure 1. Overview of the resilience hub siting and design methodology.

The paper is organized as follows: Section 2 provides background on resilience hubs. Section 3 presents the methodology for siting resilience hubs. Section 4 discusses the methodology for designing the energy systems of resilience hubs. Section 5 applies the proposed methodologies to a case study in Salt Lake City, UT, and Section 6 draws the conclusions.

2. Resilience Hubs: Providing Community and Power Grid Resilience

Resilience hub is a community-oriented facility designed to provide physical resilience, promote social well-being, and provide flexible and versatile power resources to communities and the grid [12, 13]. The key features of resilience hubs are: community alignment, resilient energy system, safe and accessible building structures, and the ability to provide community resources and services during all times. During heat waves, the resilience hubs can provide a safe cooling area with reliable electricity, even during outages.

Resilience hubs have been implemented in several cities across the U.S. Baltimore, Maryland, has a city-run Community Resiliency Hub Program with 16 sites at trusted community locations to serve under-served neighborhoods throughout the region, each outfitted with solar PV and energy storage to provide reliable emergency response during disasters [14]. A review of existing resilience hubs discussed different methods of meeting accessibility needs through transportation and current shortcomings in [15]. A study to inform the implementation of a resilience hub in Detroit, Michigan, identified community-specific vulnerabilities to climate change and provided recommendations in [16]. A high-level discussion for siting resilience hubs based on regional vulnerabilities to extreme weather events in Maui, Hawai'i is presented in [17]. Here, we take a step further and apply an analytical framework to site and design resilience hubs to meet the needs of a community vulnerable to extreme weather events.

3. Siting a Resilience Hub

This section presents a resilience hub siting framework that quantifies community vulnerability to heat waves using environmental and community factors. The proposed model identifies an ideal resilience hub location among available public buildings based on community vulnerability, as depicted in Fig. 2, and discussed in detail next.

3.1. Assessing Community Vulnerability to Heat Waves

A community's vulnerability to heat waves, V_c, is directly related to its susceptibility to heat waves, S_c,

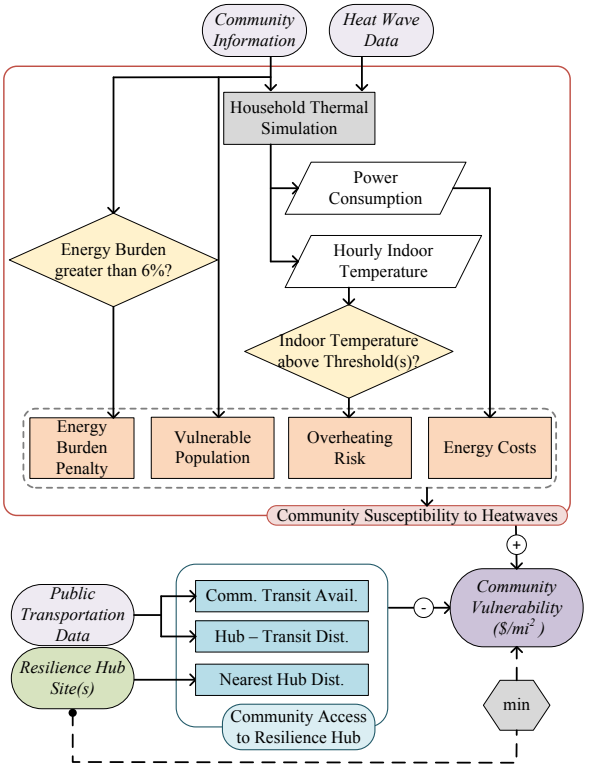

Figure 2. The proposed resilience hub siting framework

and its access to resilience services, A_c. This dynamic is defined in (1):

$$V_c = S_c - A_c, \tag{1}$$

where larger community susceptibility to heat waves increases vulnerability; meanwhile, enhanced access to resilience services decreases it. This uses a similar approach to the concept of social burden, defined in [18].

Community susceptibility considers the existing community condition and socioeconomic makeup to measure the potential adverse effects of a heat wave. This paper identifies four key considerations to characterize a community's susceptibility to heat waves: air conditioning energy consumption, indoor air temperature, prominence of vulnerable individuals, and average community energy burden. We assign cost values to each of the considerations to compare communities' vulnerabilities across a region. The diagram for this process is shown in Fig. 2.

3.1.1. Modeling Air Conditioning Requirements: A household's air conditioning (AC) system's ability to maintain indoor temperatures at acceptable levels is a key factor in quantifying community susceptibility. During heat waves, an AC system may be unable to maintain indoor air temperatures even at full output. This paper models the energy consumed by AC at time t for household archetype h in community c, $P^{ac}_{c,h,t}$, as an equivalent RC model where thermal resistance $R_{c,h}$ and capacitance $C_{c,h}$ dictate the home's thermal properties, as in [6]. Considering the thermal resistance and capacitance, AC system operation, and outdoor temperature $\theta^{out}_{c,t}$ at time t, and the local heating effects for community c, the indoor temperature $\theta^{in}_{c,h,t}$ can be calculated. These dynamics are defined in (2)-(3):

$$P^{ac}_{c,h,t} = \frac{\theta^{out}_{c,t} - \theta^{set}_{t}}{CP_{c,h}R_{c,h}}, \tag{2}$$

$$\theta^{in}_{c,h,t} = a_h\theta^{in}_{c,h,t-1} - b_h CP_{c,h}P^{ac}_{c,h,t} + f_h\theta^{out}_{c,t-1}. \tag{3}$$

The energy consumption of the AC system is defined in (2), where θ^{set}_t is the thermostat setpoint, and $CP_{c,h}$ is the AC system coefficient performance for household h in community c. The internal temperature of household archetype h at time t in community c is defined in (3), where $a_h = 1 - \Delta t/(R_hC_h)$, $b_h = \Delta t/C_c$, and $f_c = \Delta t/(R_cC_c)$. The AC system is assumed to have a maximum output.

Households in the same archetype have similar thermal properties and coefficients of performance for their AC systems. This allows community AC power consumption to be characterized based on the prominence of a given household archetype. The total AC system energy consumption across a community, P^{ac}_c, considering the home archetypes is defined in (4), where $\rho^{ac}_{c,h}$ is the proportion of archetype h in community c:

$$P^{ac}_c = \sum_{t=1}^{T}\sum_{h=1}^{H} \rho^{ac}_{c,h}P^{ac}_{c,h,t}. \tag{4}$$

3.1.2. Indoor Air Temperature Thresholds: When indoor temperatures are too high for a sustained period of time, the risk of heat-induced illnesses increases significantly, especially in elderly populations [2]. Therefore, a penalty is levied in the community susceptibility calculation if the indoor temperature exceeds a threshold. This work defines two indoor temperature thresholds as in [6]. The value of added risk by exceeding these thresholds is defined in (5)-(6):

$$S^{over}_{c,h} = \begin{cases} \sum_{t'=1}^{\tau_1} \alpha^{over}_1, T^{over}_1 \le \theta^{in}_{c,h,t} < T^{over}_2 \\ \sum_{t'=1}^{\tau_2} \alpha^{over}_2, \quad T^{over}_2 \le \theta^{in}_{c,h,t} \end{cases}, \tag{5}$$

$$S_c^{over} = \sum_{h=1}^{H} \rho_{c,h}^{ac} S_{c,h}^{over}. \quad (6)$$

The total cost of exceeding internal temperature thresholds $S_{c,h}^{over}$ for household h in community c is defined in (5), where α^{over} is the penalty in \$ for exceeding the threshold for a given time step, T^{over} is the temperature threshold, τ_1 is the number of occurrences of $T_1^{over} \leq \theta_{c,h,t}^{in} < T_2^{over}$, and τ_2 is the number of occurrences of $T_2^{over} \leq \theta_{c,h,t}^{in}$. It is assumed $\alpha_2^{over} > \alpha_1^{over}$. The total community cost is found by aggregating across all household archetypes in (6).

3.1.3. Considering community socioeconomics: The average energy burden and proportion of vulnerable people (above 65 years of age or with registered disabilities) are considered in measuring susceptibility to heat waves in (7)-(8). The cost of the prominence of vulnerable individuals in community c, S_c^{vuln}, is defined in (7), where ρ_c^{vuln} is the proportion of households with a vulnerable member, and α^{vuln} is the assigned penalty:

$$S_c^{vuln} = \sum_{h=1}^{H} \rho_c^{vuln} \alpha^{vuln}. \quad (7)$$

If the community has an average energy burden B_c greater than a threshold T^{burd}, the energy burden cost S_c^{burd} is applied based on the penalty α^{burd} in (8):

$$S_c^{burd} = \begin{cases} \alpha^{burd}, & B_c \geq T^{burd} \\ 0. & B_c < T^{burd} \end{cases}. \quad (8)$$

3.1.4. Total community susceptibility: The total susceptibility for community c is calculated for two scenarios during a heat wave: normal power grid conditions, scenario n, and a power outage during hours 17-20, scenario o. The susceptibility cost is calculated for each scenario in (9)-(10):

$$S_c^n = \pi^e P_c^{ac,n} + S_c^{over,n} + S_c^{vuln} + S_c^{burd}, \quad (9)$$

$$S_c^o = \pi^e P_c^{ac,o} + S_c^{over,o} + S_c^{vuln} + S_c^{burd}. \quad (10)$$

In each, the cost of energy $\pi^e P_c^{ac}$ and overheating penalty S_c^{over} depend on the outage conditions. The full community susceptibility cost S_c for a heat wave is defined in (11):

$$S_c = P_c^{dens}\left(w^n S_c^n + w^o S_c^o\right), \quad (11)$$

where P_c^{dens} is the population density of community c, and w is the weight parameters for each scenario. The weight parameters w allow the susceptibility cost to reflect the likelihood of outages during extreme weather events. Different methods can be used to assign penalty costs when defining susceptibility. For example, the penalty for dangerously high indoor air temperatures can be based on resulting medical costs if high-induced illnesses were to occur. These values should be regionalized and informed by local demographics and data. Nonetheless, in this application, the penalties inform a rank-based system, serving as weights that can be tuned to the comparative susceptibility between communities.

3.2. Siting Optimization Model

The siting optimization model minimizes community vulnerability by choosing resilience hub locations from a discrete set that provides the greatest access values.

3.2.1. Community Access to Resilience: Community access to resilience (A_c) is a measure of a community's ability to relocate to a resilience hub and is characterized by the community's proximity to the hub and its local access to public transit. Without access to resilience hubs, community vulnerability equals community susceptibility, that is $A_c = 0$. The services a resilience hub can provide increase substantially as it comes within walking distance or is easily accessible by public transportation. Therefore, the value of community access increases non-linearly as proximity to the hub and availability of public transportation increase, as defined in (12):

$$A_c = aR, \quad (12)$$

where R is the generic value of added resilience from resilience hub h, and a is a coefficient classified by the accessibility of the resilience hub h to community c. The generic resilience value should be defined in relation to how the features of the resilience hub address community vulnerability. Perfect access (meaning $a = 1$) to an optimally designed resilience hub can mitigate all of a community's heat wave susceptibility, so here $R = S_c$. A_c is scaled by $a \in [0, 1]$, a set of coefficients defined to reflect varying levels of accessibility.

3.2.2. Minimizing Community Vulnerability: The vulnerability of community c to heat waves considering their access to resilience A_c is calculated for each possible resilience hub location l as $V_{c,l}^{hub}$.

Then, a mixed-integer linear programming problem identifies the optimal deployments of resilience hubs at pre-defined sites as defined in (13)-(16). The objective function (13) minimizes the sum of community vulnerability across a region C based on deploying resilience hubs at discrete sites:

$$min \quad \sum_{c=1}^{C}\sum_{l=1}^{L} V_{c,l}^{hub} I_{c,h}^{n}, \tag{13}$$

where $I_{c,l}^{n}$ is a binary variable associated with the closest resilience hub to community c. The model is constrained to (14)-(16):

$$I_{c,l}^{n} \leq I_{l}, \tag{14}$$

$$\sum_{l=1}^{L} I_{l} = N^{hubs}, \tag{15}$$

$$\sum_{l=1}^{L} I_{c,l}^{n} = 1. \tag{16}$$

Each community has access to the same hub locations, defined in (14), where I_l is the binary status of a resilience hub at location l. The total number of hubs to be sited is defined in (15), where N^{hubs} is the number of hubs. Community vulnerability only considers its most accessible hub, constrained in (16).

4. Designing a Resilience Hub

There are several factors to consider when designing the components of a resilience hub. This section presents general approaches to sizing the hub, the AC system to meet indoor temperature requirements, and the associated energy system to provide the hub with sufficient power during heat wave-induced outages.

4.1. Capacity Assessment and AC Sizing

Emergency shelters have a spatial occupancy limit. The American Red Cross suggests emergency shelters be capable of hosting 25% of their surrounding population with a minimum of 10 sqft available to each person. This work uses the same parameters to assess the capacity of a resilience hub. The hub capacity can be defined by evaluating community populations and the number of hubs available in the region.

The method defined in Section 3.1.1 is used to simulate the resilience hub's internal temperatures and define the AC system power requirements The thermal resistance is scaled to correlate to the larger building area for the thermal simulation of the resilience hub. The output of the thermal simulation provides the AC system load profile for the hub during the heat wave. This work does not consider improving the thermal resistance or capacitance of the hub.

4.2. Energy System Sizing

The energy system must provide sufficient power to meet the resilience hub's load during outage conditions for extended periods of time. Resilience hubs are most commonly outfitted with solar PV and energy storage systems (ESS), as they provide clean onsite generation and storage and are typically in line with community sustainability goals. However, different outage scenarios may necessitate differing solar PV and ESS capabilities based on varying load and solar irradiance. The methodology to size a resilience hub under various outage conditions is presented in Fig. 3.

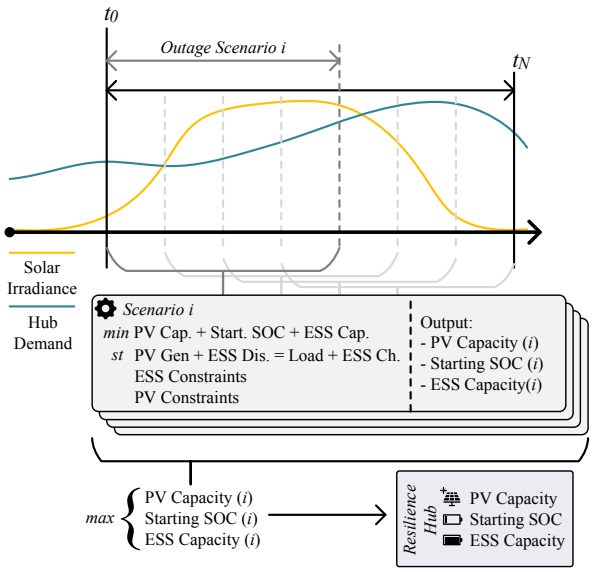

Figure 3. The proposed method for sizing the energy system of resilience hubs

An MILP model is defined in (17)-(24) to determine the minimum solar PV system capacity, baseline ESS state-of-charge (SOC), and ESS capacity to meet a resilience hubs energy needs during any number of outage scenarios. The objective function seeks to minimize the capital expenditure associated with deploying the necessary solar PV and ESS system and minimize the energy costs of baseline ESS SOC in (17):

$$min \quad \pi^{pv}\mathcal{C}^{pv} + \lambda\mathcal{ESS}_0 + \pi^{ess}\mathcal{C}^{ess}, \tag{17}$$

where $\mathcal{C}^{pv}$ is the capacity of the solar PV (in kW), $\mathcal{C}^{ess}$ is the capacity of the ESS (in kWh), $\mathcal{ESS}_0$ is the SOC of the ESS at $t = 0$, π is the capital expenditure cost for each asset (in \$/kW and \$/kWh, respectively), and

λ is the retail energy cost. The objective function is constrained by (18)-(24):

$$P_{i,t}^{pv} + P_{i,t}^{ess,d} = L_t + P_{i,t}^{ess,c}, \quad (18)$$

$$P_{i,t}^{pv} = C_i^{pv} n_t^{pv}, \quad (19)$$

$$ESS_{i,t} = ESS_{i,t-1} + \eta P_{i,t}^{ess,c} - \frac{1}{\eta} P_{i,t}^{ess,d}, \quad (20)$$

$$0 \leq ESS_{i,t} \leq C_i^{ess,max}, \quad (21)$$

$$0 \leq P_{i,t}^{ess,c} \leq \epsilon C_i^{ess} I_{i,t}^{ess,c}, \quad (22)$$

$$0 \leq P_{i,t}^{ess,d} \leq \epsilon C_i^{ess} I_{i,t}^{ess,d}, \quad (23)$$

$$I_{i,t}^{ess,c} + I_{i,t}^{ess,d} \leq 1, \quad (24)$$

$$\mathcal{C}^{pv} \geq C_i^{pv}, \quad (25)$$

$$\mathcal{C}^{ess} \geq C_i^{ess}, \quad (26)$$

$$\mathcal{ESS}_0 \geq ESS_{i,0}, \quad (27)$$

$$\sum_{t=1}^{T} \mathcal{C}^{pv} n_t^{pv} \geq \mathcal{ESS}_0. \quad (28)$$

Resilience hub load balance is asserted in (18), where $P_{i,t}^{pv}$ is the solar PV generation, $P_{i,t}^{ess,d}$ is the ESS discharge, L_t is the resilience hub load, which is generated by the resilience hub AC system operations and a buffer to compensate for additional demand, and $P_{i,t}^{ess,c}$ is the ESS charge, all at time t for outage scenario i. PV generation is defined in (19), where C_i^{pv} is the solar PV capacity for outage scenario i, and n_t^{pv} is the normalized solar irradiation at time t. This optimization assumes perfect solar forecasts with the maximum $n_t^{pv} = 1$. Energy storage operational parameters are defined in (21)-(24), where η is the efficiency of the ESS, ϵ is the power-to-energy ratio of the ESS, and $I_{i,t}^{ess,d}$ and $I_{i,t}^{ess,c}$ are binary variables associated with the ESS discharging and charging states. Decomposition techniques can be used to ensure (22)-(23) are linear. The minimum capacity of solar PV, ESS SOC, and ESS initial charge to satisfy hub load balance for each outage scenario is defined (25)-(27). Finally, the solar PV generation through one day must be capable of charging the battery to its baseline initial state, defined in (28). Note, solar PV generation deviating from its original forecast can be compensated by raising the minimum ESS capacity to have contingency reserves.

This work assumes backup diesel generators may be used to counteract intermittent renewable generation. The capacity requirements for backup generation if the resilience hub is to run continuously are defined in 29:

$$C^{diesel} = max\{L_t\}, \quad (29)$$

where C^{diesel} is the maximum power output of the backup generator. The fuel storage requirements for the backup generator are defined in (30), where G^{disel} is the total amount of fuel that must be stored, and ϕ is the backup generator fuel consumption parameter:

$$G^{diesel} = \phi\big(\sum_{t=1}^{T} L_t - ESS_0\big). \quad (30)$$

5. Case Study

5.1. Modeling Community Vulnerability in Salt Lake City

Salt Lake City (SLC), Utah, experiences heat waves annually. For this study, communities in SLC are classified by U.S. census tracts. Temperature data from July 22, 2023 for SLC is used. The urban heating effect for census tracts in SLC is obtained from [19]. U.S. Census Bureau American Community Survey (ACS) data is used to characterize the susceptibility of census tracts in SLC to heat waves. Household archetypes depend on structure (stand-alone or apartment) and primary energy source. It is assumed that apartments generally have more favorable thermal properties, and electricity as a primary energy source correlates to higher coefficients of performance. Table 1 defines the parameters for community thermal simulations. The associated penalties, weights, and thresholds used in calculating susceptibility are defined in Table 2. Indoor overheating thresholds are based on values defined in [6]. ACS data is used to quantify the size of proportion of household archetypes, vulnerable populations, and the average energy burden per census tract.

Table 1. Household Archetype Parameters

	1	2	3	4
Thermal Res., R (kWh/°C)	3	3	1.75	1.75
Thermal Cap., C (°C/kW)	3	3	1.75	1.75
Coeff. of Perf., CP	1	0.8	1	0.8
Max Output, P^{hvac} (kW)	4	4	4	4

The vulnerability assessment results are presented in Fig. 4. The effects of heat waves are exacerbated in central areas of SLC due to urban heating effects (Fig. 4a). This results in the spatial distribution of community vulnerability seen in Fig. 4b, which finds the most vulnerable communities are those in central SLC. Central SLC is the most urbanized, with limited shade from tree coverage and generally low surface albedo, increasing heating effects. Similarly, households in western SLC have relatively high urban heating effects and lower incomes, increasing their vulnerability.

Table 2. Susceptibility Parameters

Variable	Value	Unit
α_1^{over}	50	\$
α_2^{over}	200	\$
α^{vuln}	100	\$
α^{burd}	100	\$
π^e	0.09	\$/kWh
T_1^{over}	27	°C
T_2^{over}	32	°C
T^{burd}	6	%
w^n	0.5	-
w^o	0.5	-

Wealthy communities are largely located in higher elevations (along east SLC) with proportionately cooler temperatures and generally have better access to HVAC.

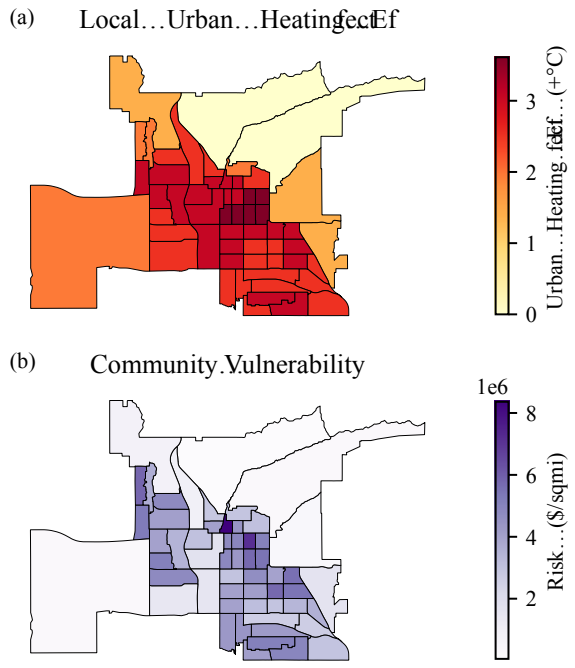

Figure 4. (a) Community urban heating effect, and (b) Community vulnerability, in Salt Lake City, UT

5.2. Siting Resilience Hubs in Salt Lake City

5.2.1. Community Access to Resilience: The geometric center of each census tract is used to measure its distance from hub locations. For this case study, the accessibility coefficient, a, can take on four values according to the criteria in Table 3. If a resilience hub is within walking distance of the geometric center of the tract, it provides the highest practical access to resilience. If a hub is within a defined distance of a public transit stop and there are sufficient stops within a tract, we conclude it provides higher access to resilience than driving. Note we assume proximity to light-rail stations provides higher accessibility than bus stops alone, as light-rails run more frequently than most bus routes in SLC.

Table 3. Access to Resilience Hub coefficients

Mode	Criteria	Value
Walking	$\leq$ 0.5 mi to hub site	0.99
Transit (bus only)	$\geq$ 20 bus stops/mi^2	0.3
Transit (bus+light-rail)	$\geq$ 20 bus stops/mi^2 + light-rail stop $<$ 0.25 mi from hub site	0.8
Driving	$<$ 20 mi to hub site	0.1

5.2.2. Siting Hubs to Reduce Vulnerability: The formulation proposed in Section 3.2.2 is applied to the eight public libraries in SLC (Fig. 5a). The model was run for a case of siting a single hub and one for three. In the first case (Fig. 5b), the hub is deployed at the central library location. This hub is closest to the most vulnerable communities in SLC, and it also has a dedicated light-rail station, providing access for many surrounding communities. For three hubs (Fig. 5c), sites are located at additional vulnerability hotspots. Despite high local vulnerability, a resilience hub is not deployed at the northwest site because there are limited public transit opportunities, decreasing its accessibility.

5.3. Resilience Hub Design in Salt Lake City

5.3.1. Capacity Considerations: A capacity analysis for resilience hubs located at all eight of the public libraries in SLC was applied based on the building square footage and the population of the closest census tracts, presented in Table 4. The analysis found a total capacity deficit of over 23,000 people, highlighting the need for additional community centers to host resilience hubs. Enrolling public schools or local religious centers could supply extra capacity. However, not all people are likely to have insufficient AC systems, reducing the severity of the capacity deficit.

5.3.2. AC System Sizing: The thermal features and energy systems sections of the remainder of the case study both consider a hypothetical resilience hub in SLC. The theoretical hub is one of eight, each having a capacity for 7,091 people and a square footage of 70,905 sqft. The thermal resistance of the building is scaled to reflect the increase in surface area of the building envelope. Three AC systems are tested: a conventional centralized duct system (Conv. Cen.), an air-source heat pump system (Air Src. HP), and a geothermal heat

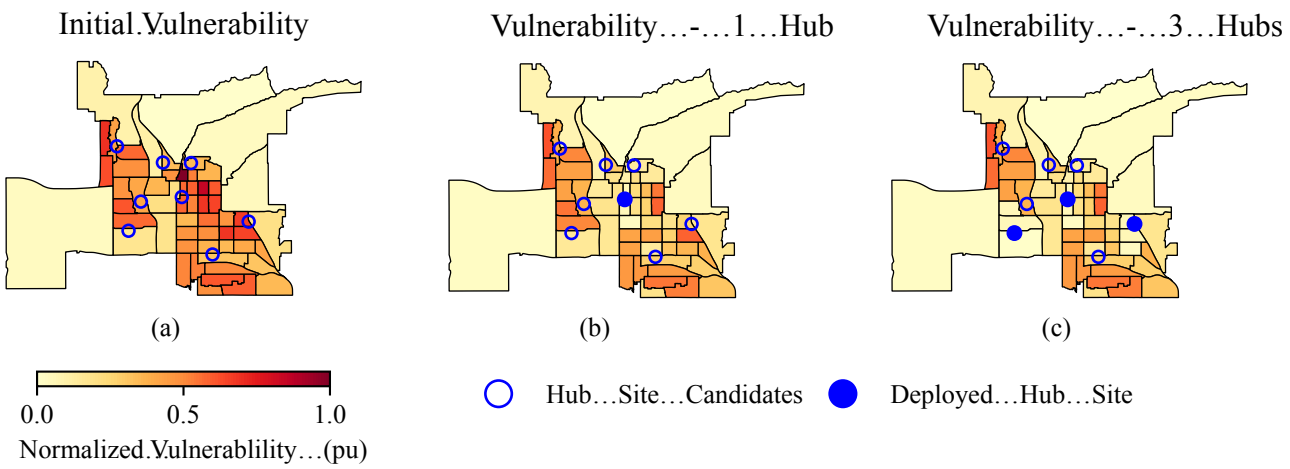

Figure 5. Census tract-level risks (a) before resilience hub deployments, (b) after one resilience hub deployment, (c) after three resilience hub deployments

pump system (Geo. HP). The operation of each AC system during a heat wave is presented in Fig. 6. In each case, the peak outdoor temperatures correlate to the maximum energy consumption, but the CP (see Table 5) significantly impacts the operation of each system. Improved CP values significantly reduce the peak power consumption for the AC systems. From this, the required capacity and expected capital expenditure are reported in Table. 5. Unit costs were generated from quotes of commercial units meeting the required capacity. Expenditure increases as the CP improves despite the capacity requirements of the AC system decreasing with high CP values.

Table 4. Capacity Analysis for Resilience Hubs at Public Libraries in SLC

Hub Location	Area (1k sqft)	Pop. to Serve (1,000's)	Capacity Deficit (1,000's)
Day-Riverside	13.0	9.2	7.9
Marmalade	18.6	4.4	2.6
Sweet	8.0	5.1	4.3
Main	240.0	10.7	-13.3
Chapman	8.9	8.9	8.1
Glendale	20.0	2.8	0.7
Sprague	13.0	11.7	10.4
Anderson-Foothill	14.9	3.9	2.4
Total	328.4	56.7	23.9

5.3.3. Energy System Design: Eight outage scenarios were applied to the model defined in Section 4.2, each lasting four hours, starting each hour between 10:00 and 18:00. This is a conservative estimation as SLC typically experiences a total of 2-3 non-consecutive hours of power outages per year [20]. Each solar panel

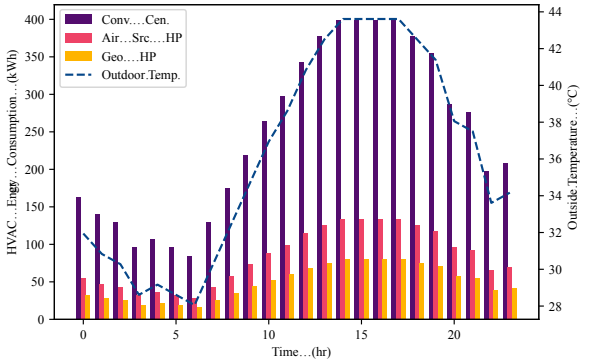

Figure 6. Resilience hub AC system performance for different systems

is assumed to have a 400 W capacity and is 79" by 39" in size. Assuming the resilience hub has three floors equally dividing the square footage, the rooftop has enough area for a solar capacity of 441.9 kW. Capacity costs of solar are $1,291/kW for rooftop installations, $1,754/kW for parking canopy installations, and capacity costs of ESS are $2,500/kWh, both based on values in [21]. The energy storage cost is valued based on SLC residential rate tariffs at $0.09/kWh. The ESS is assumed to have a 0.15 power-to-energy ratio. Backup system capacity parameters are assumed to be $150/kW, $3.50/gal., operating at 10 kWh/gal., and storage tank costs are estimated based on industry quotes. The model was applied to each of the three AC system cases.

The energy system required to balance hub demand during outages for each AC system scenario is displayed in Table 5. Solar PV installation is preferred as it has a lower capital cost, but it is limited by its variability. Higher AC system load requires greater capacity of

both solar PV and ESS. Despite a significantly lower AC system capital expenditure, the total expenditure for the Conv. Cen. AC system is significantly greater than the other two cases due to high solar PV and ESS requirements. The Geo. HP case has over double the cost for its AC system installation, but the decreased AC load reduces total costs compared to other cases. The Conv. Cen. and Air Src. HP configurations required larger solar capacity than the rooftop could accommodate, leading to additional parking canopy installations. Lower AC system loads also allow for smaller backup diesel systems with lower costs. However, even the largest backup diesel system only marginally contributes to the total system cost.

Table 5. Resilience Hub ESS + Solar PV Energy System Outage Analysis Results

Energy System Component		Conv. Cen.	Air Src.	Geo. HP
AC System	CP	1	3	5
	Peak (kW)	399.5	133.2	79.9
	CAPEX ($M)	0.17	0.49	1.09
Solar PV	Cap. (kW)	1,298	542.2	392.8
	CAPEX ($M)	2.07	0.75	0.51
Energy Storage	Cap. (MWh)	2.18	0.90	0.65
	SOC (MWh)	1.10	0.46	0.33
	CAPEX ($M)	5.45	2.26	1.62
Total CAPEX ($M)		11.15	3.50	3.22
Backup Diesel	Cap. (kW)	439.5	173.2	119.9
	Str. (gal.)	578.4	247.2	181.0
	CAPEX ($M)	0.10	0.04	0.02
Total + Backup ($M)		11.2	3.5	3.2

A more in-depth analysis of the energy system sizing model per each outage scenario under the Conv. Cen. AC system case is displayed in Fig. 7. The capacity of the ESS system is influenced heavily by the last three evening and night outage scenarios (scenarios 6-8). Solar PV is limited in each of these scenarios due to limited irradiance, so the ESS is more heavily relied upon, increasing the necessary rated capacity to meet demand. Considering this, it may be more economical to size up backup diesel generation rather than to completely rely on ESS discharge.

Finally, the energy system is simulated over three days during a heat wave without outages. Heat waves can often last multiple days, but it is highly unlikely outages will persist for the full duration. The hub must not cause added strain on the grid during extreme events, and if possible, it should offer additional flexibility and resilience. As can be seen in Fig. 8, the resilience hub can operate fully without incurring system demand and can export power to support other neighboring loads.

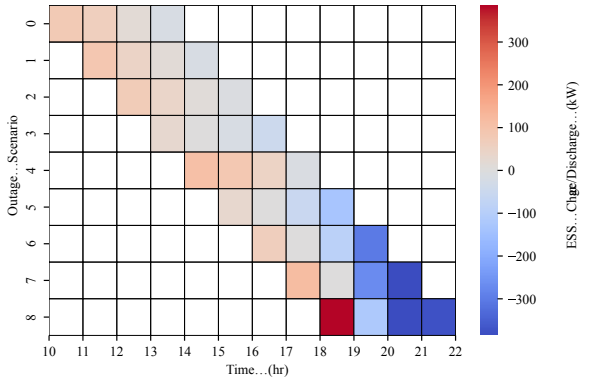

Figure 7. ESS performance for different outage start time scenarios during a heat wave

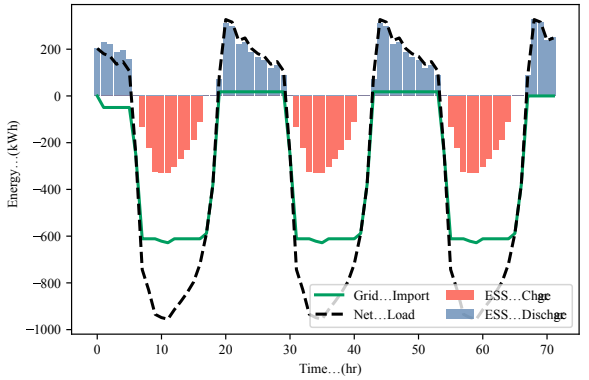

Figure 8. Resilience hub energy system operation during heat wave without an outage

The solar PV generation is significantly larger than the hub demand, allowing the hub to export to the grid during daytime hours while concurrently charging the ESS, and discharge to meet hub load at night.

6. Conclusion

Worldwide, climate change is increasing the severity of heat waves, burdening communities with increased heat-related illnesses and the power grid with growing peak system demand. This paper develops a framework for siting and designing resilience hubs to mitigate these effects. It characterized community-specific vulnerability to heat waves given socioeconomic information, indoor temperature simulations, and urban heating effects across Salt Lake City. This informed an optimal resilience hub deployment at public library locations across the region to strategically minimize the vulnerability of communities. In addition, this work defined a method to size a resilience hub's energy systems to provide the hub with sufficient power during

heat wave-induced outages. This work also evaluated the different costs associated with different AC and energy system configurations for the hubs. This work serves as a tool for local governments to develop resilience to heat waves in a more targeted manner. It also provides a generic approach for organizations to develop resilience hubs that are formally designed to provide uninterrupted services to communities in need while enhancing grid resilience.

References

[1] Dana Habeeb, Jason Vargo, and Brian Stone. "Rising heat wave trends in large US cities". en. In: *Natural Hazards* 76.3 (2015), pp. 1651–1665.

[2] S. Tham et al. "Indoor temperature and health: a global systematic review". en. In: *Public Health* 179 (2020), pp. 9–17. ISSN: 00333506.

[3] Seth Borenstein. "2023 set a record for U.S. heat deaths. Why 2024 could be even deadlier". en. In: *PBS* (2024).

[4] Shuchen Cong et al. "Unveiling hidden energy poverty using the energy equity gap". en. In: *Nature Communications* 13.1 (2022), p. 2456.

[5] T Chakraborty et al. "Disproportionately higher exposure to urban heat in lower-income neighborhoods: a multi-city perspective". en. In: *Environmental Research Letters* 14.10 (2019), p. 105003.

[6] Luis Rodriguez-Garcia, Miguel Heleno, and Masood Parvania. "Assessing the Impacts of Power Outage on Community Overheating Risk during Extreme Heat Waves". en. In: *HICCS* (2023).

[7] L. Rodriguez-Garcia, M. Heleno, and M. Parvania. "Power Distribution System Planning for Mitigating Overheating Risk Inequity". In: *IEEE Transactions on Power Systems* (2024).

[8] David J. Sailor. "Risks of summertime extreme thermal conditions in buildings as a result of climate change and exacerbation of urban heat islands". en. In: *Building and Environment* 78 (2014), pp. 81–88.

[9] Vivian Do et al. "Spatiotemporal distribution of power outages with climate events and social vulnerability in the USA". en. In: *Nature Communications* 14.1 (2023), p. 2470.

[10] Jesse Dugan and Salman Mohagheghi. "Assessment of Social Vulnerability to Long-Duration Power Outages in the United States". en. In: *2023 IEEE GreenTech*. Denver, CO, USA: IEEE, Apr. 2023, pp. 123–127.

[11] Bethel Tarekegne et al. "Assessing the Energy Equity Benefits of Energy Storage Solutions". en. In: *2022 EESAT Conference*. Austin, TX, USA: IEEE, Nov. 2022, pp. 1–5.

[12] Kristin Baja. *Resilience Hubs: Shifting Power to Communities and Increasing Community Capacity*. Tech. rep. Urban Sustainability Directors Network, 2018.

[13] Alex Farley, Hollis Belnap, and Masood Parvania. "Resilience Hubs: Bolstering the Grid and Empowering Communities". In: *IEEE Power and Energy Magazine* 22 (July 2024), pp. 38–48.

[14] Aubrey Germ. *The Baltimore City Community Resiliency Hub Program*. 2024. URL: https://www.baltimoresustainability.org/baltimore-resiliency-hub-program/.

[15] Thayanne G.M. Ciriaco and Stephen D. Wong. "Review of resilience hubs and associated transportation needs". en. In: *TRIP* 16 (Dec. 2022), p. 100697.

[16] Maegan Muir et al. *Detroit Resilience Hub Framework*. Tech. rep. University of Michigan School for Environment and Sustainability, 2022.

[17] A. F. de Roode and I. Martinac. "Resilience hubs: a Maui case study to inform strategies for upscaling to resilience hub networks across coastal, remote, and island communities". en. In: *IOP Conference Series: Earth and Environmental Science* 588.5 (Nov. 2020), p. 052050.

[18] Susan Clark et al. "Developing an equity-focused metric for quantifying the social burden of infrastructure disruptions". en. In: *Sustain. and Resilient Infrastruct.* 8 (2023), pp. 356–369.

[19] Maegan Muir et al. *Salt Lake City, Utah, Heat Watch Report*. Tech. rep. CAPA Strategies, 2023.

[20] *Annual Electric Power Industry Report*. 2023. URL: https://www.eia.gov/electricity/data/eia861/.

[21] *2023 Electricity ATB Technologies and Data Overview*. 2023. URL: https://atb.nrel.gov/electricity/2023/index.